Reconstruction of turbulence parameters under strong scintillation

A.S. Gurvich and O.V. Fedorova

A.M. Obukhov Institute of Atmospheric Physics, Moscow

Received July 30, 2007

Spatial spectra of strong scintillation behind a phase screen with isotropic heterogeneities have been studied. The medium forming the screen was described by the Kolmogorov 3D spectrum of heterogeneities. Calculations were performed for conditions of optical observations through the Earth's atmosphere from a satellite. The domains of applicability for three different approximations of the solution of the equations for 2D spectra have been studied; the possibility to determine medium parameters from the observed 1D spectra of strong scintillation is investigated; and the domain of measured parameters, which contains the solution for the inverse problem stable with respect to measurement errors, has been determined.

Introduction

It is commonly accepted that it is very difficult to determine turbulence characteristics from observations of strong saturated scintillation.[1] Approximation of weak scintillation is successfully used in reconstruction of turbulence parameters on the base of satellite observations of stars through the Earth's atmosphere.[2,3] Applicability limits of such approximation were defined more exactly in Ref. 4 for determining parameters of anisotropic heterogeneity generated by internal waves in the atmosphere. In this paper we study the possibility to determine parameters of the locally isotropic turbulence from measurements of strong scintillation spectra. The problem is posed as applied to conditions, under which the turbulent medium is localized at a long distance from the observation plane.

The study is based on numerical computations with the model of phase screen. The model is widely used in investigations of scintillation generated by heterogeneity of the interplanetary medium and atmospheres of planets, including the atmosphere and ionosphere of the Earth. For the phase screen model, there exist integral relations connecting scintillation spectra with spectra of phase fluctuations on the screen.[5] The latter, in turn, are defined by fluctuation spectra of the refractive index of the medium, through which the wave is propagated. The integral relations in their general form were introduced by V.I. Shishov.[6,7] They form the fundament for numerical simulation of initial data, which are necessary for solving the inverse problem. In this part, our study is contiguous with Ref. 8, presenting the numerical analysis of intensity fluctuations behind Kolmogorov's phase screen, and with Refs. 9 and 10, dealing with two-dimensional scintillation spectra behind an isotropic power phase screen with a spectrum, characterized by a small (as compared to Fresnel scale) internal scale and different indices between 2 and 6 at the power part.

Note that the theoretical study of strong scintillation is still a matter of interest.[11–13] This is connected with quickly growing applications of satellite methods to sounding the Earth's atmosphere, which are based on sensing by optical and radiowaves.[14–18]

In this paper we consider spatial spectra of strong scintillation observed behind a phase screen with isotropic heterogeneities compared with the Fresnel scale and of a less scale. For definiteness, parameters of the problem are chosen so that they correspond to conditions of optical observations through the Earth's atmosphere from a satellite. Different approximations are compared with exact calculations of 2D spectra. In combination with common approximations, we use an asymptotic formula proposed in Refs. 12 and 13 for the long-wave part of the spectrum. In addition to the direct problem, i.e., calculation of scintillation spectra by given characteristics of the medium, we consider the inverse problem: determining parameters of the medium by observed 1D spectra.

Theory

The model of a flat phase screen[19] was constructed under the assumption that the screen is formed by a layer of a turbulent medium with Kolmogorov's spectrum of fluctuations of the refractive index n [Ref. 20]:

$$\Phi_n(\mathbf{k}) = \frac{\Gamma(8/3)\sin(\pi/3)}{4\pi^2} C_n^2 k^{-11/3} \exp\left(\frac{-k^2}{\kappa_m^2}\right),$$
$$k^2 = k_x^2 + k_y^2 + k_z^2, \qquad (1)$$

where C_n^2 is a structural characteristic that defines power of fluctuations; $\mathbf{k}$ is the wave vector; κ_m is the wave number that defined the internal scale. In the model of a phase screen, the main part is played by the efficient structural characteristic $C_{\text{ef}}^2 = C_n^2 L_{\text{t}}$, where L_{t} is the equivalent thickness of the phase screen.

The two-dimensional spectral density of scintillation F_I is defined by the equations[6,7]

0235-6880/08/02 96-06 $02.00

$$\mathrm{F}_I(k_z,k_y)=\frac{1}{4\pi^2}\int\limits_{-\infty}^{\infty}\mathrm{d}z\mathrm{d}y\left\{\exp\left[-\Psi\left(z,y,\frac{Lk_z}{k_0},\frac{Lk_y}{k_0}\right)\right]-1\right\}\times$$

$$\times\exp\left(-i(k_z z+k_y y)\right); \qquad (2)$$

$$\Psi(z,y,z',y')=D_S(z,y)+D_S(z',y')-$$

$$-\frac{1}{2}\left[D_S(z+z',y+y')+D_S(z-z',y-y')\right], \qquad (3)$$

where $D_S(z,y)$ is the structural function of fluctuations of a wave's phase at the exit of the screen. For the model (1), the expression for the structural function is known[20]:

$$D_S(R)=\frac{6}{5}\Gamma\left(\frac{1}{6}\right)\Gamma\left(\frac{8}{3}\right)\sin\frac{\pi}{3}k_0^2C_{\mathrm{ef}}^2\kappa_m^{-5/3}\times$$

$$\times\left[M\left(-\frac{5}{6},1,-\frac{R^2\kappa_m^2}{4}\right)-1\right], \qquad (4)$$

where $k_0=2\pi/\lambda$ is the wave number of light; M is the confluent hypergeometric function.

For the isotropic case, $F_I=F_I(K)$, $K^2=k_z^2+k_y^2$. An important characteristic of a stochastic field behind the screen is the coherence function $\Gamma_2(\mathbf{R})=\exp[-D_S(\mathbf{R})/2]$, $\mathbf{R}=\{z,\ y\}$.[5]

Just as in Refs. 4, 12, and 13, dispersion of scintillation β_0^2 calculated in the approximation of weak scintillation[20] in the observation plane at the distance L from the screen was chosen as a parameter characterizing the scintillation intensity. For the model (1) in this approximation we obtain

$$\beta_0^2=\frac{6}{5}\Gamma\left(\frac{1}{6}\right)\Gamma\left(\frac{8}{3}\right)\sin\frac{\pi}{3}k_0^2C_{\mathrm{ef}}^2R_F^{5/3}(R_F\kappa_m)^{-5/3}\times$$

$$\times\left\{\left[1+(R_F\kappa_m)^4\right]^{5/12}\cos\left[\frac{5}{6}\arctan(R_F\kappa_m)^2\right]-1\right\}, \qquad (5)$$

where the Fresnel scale is $R_F=\sqrt{L/k_0}$.

As a rule, experiments deal with measurements of one-dimensional scintillation spectra. For the isotropic case, 1D spectra $V_I(\kappa)$ are connected with 2D spectra by the equation[20]

$$V_I(\kappa)=2\int\limits_{\kappa}^{\infty}F_I(K)\frac{K}{\sqrt{K^2-\kappa^2}}\mathrm{d}K, \qquad (6)$$

where κ is the one-dimensional wave number.

Analysis of strong scintillation ($\beta^2=\int\mathrm{d}^2\boldsymbol{\kappa}F_I(\boldsymbol{\kappa})>1$) on the base of Eq. (2) requires high calculation expenditures. Therefore, different approximations for individual domains of the 2D spectrum are used. The approximation by the spectrum of the squared coherence function Γ_2^2 for short waves[6,7]:

$$F_\Gamma(K)=\frac{1}{2\pi}\int\limits_0^{\infty}\exp\left[-D_S(\rho)\right]J_0(K\rho)\rho\,\mathrm{d}\rho, \qquad (7)$$

where J_0 is the Bessel function.

For long waves, there exists the so-called refraction approximation[6,7,10,19]

$$F_R(K)=\exp\left[-D_S\left(KL/k_0\right)\right]F_I^{(1)}(K), \qquad (8)$$

where $F_I^{(1)}(K)$ is the 2D spectrum of weak scintillation in the first approximation of the perturbation method[20]:

$$F_I^{(1)}(K)=8\pi k_0^2L_{\mathrm{t}}\Phi_n(K)\sin^2\left(\frac{LK^2}{2k_0}\right).$$

An approximate formula was proposed in Refs. 12 and 13 to describe the short-wave range of 2D spectra. The formula was obtained by decomposition of Ψ in Eq. 2 into the Taylor series by small $\{z,y\}$ in the neighborhood of the point $\{z,y\}=0$. Note that the approximation of Ψ by a square polynomial was applied earlier in Ref. 21 to calculate dispersion of strong scintillation. Here $\Psi=0$ at the point $\{z,y\}=0$, and the first term of the decomposition, which is odd in $\{z,y\}$, vanishes after integration with respect to these variables. Preserving the second term of the decomposition of the order $\{z,y\}^2$, we obtain for the model (1):

$$\Psi(z,y,K)\sim G(K)\left(w^2+k_y^2\right)+H(K)\left(k_z w+k_y v\right)^2, \qquad (9)$$

where

$$w=z/R_F^2;\quad v=y/R_F^2;\quad B=R_F^4\kappa_m^2;$$

$$A=\frac{6}{5}\Gamma\left(\frac{1}{6}\right)\Gamma\left(\frac{8}{3}\right)\sin\left(\frac{\pi}{3}\right)k_0^2C_{\mathrm{ef}}^2\kappa_m^{-5/3};$$

$$G(K)=\frac{5AB^2}{12}\left[1-M\left(\frac{1}{6},2;-\frac{BK^2}{4}\right)\right];$$

$$H(K)=\frac{5AB^2}{288}M\left(\frac{7}{6},3;-\frac{BK^2}{4}\right).$$

After substitution of Eq. 9 into Eq. 2 and integration with respect to $\{z,y\}$ we obtain an equation for the approximation F_A:

$$F_A(K)=\frac{R_F^4}{4\pi^2}\frac{48\sqrt{6}\pi\exp\left[-\dfrac{144R_F^4K^2}{5AB\left(24G+BHK^2\right)}\right]}{5AB\sqrt{G\left(24G+BHK^2\right)}}. \qquad (10)$$

Applicability limits of the approximations (7), (8), and (10) are studied below by comparison with the results of numerical integration of the equation (2).

2D scintillation spectra and their approximations

The investigations are based on numerical solution of the equation (2) for the model (1). Calculations were performed for conditions of optical observations through the Earth's atmosphere from a satellite.

Radiation wavelength λ and distance L were taken as $5 \cdot 10^{-7}$ m and 2200 km, the Fresnel scale R_F equals to 0.418 m, respectively.

The equation (5) for scintillation intensity β_0^2 includes the dimensionless wave parameter $W = R_F^2 \varkappa_m$. Its values were assigned as 2, 6, 20, 60, 200 and $W = \infty$ for the case of zero internal scale. The chosen values of W correspond to the fact that the internal scale of heterogeneity varied from the magnitude comparable with the Fresnel scale to zero. For the scintillation intensity β_0^2, we took the values of 10, 100, 1000, 10000. Totally, 24 variants of spectra were calculated. As shown in Refs. 6 and 7, the coherence radius R_C, which is defined by the equation $D_S(R_C) = 2$, is a characteristic small scale in the plane, where strong scintillation was observed. The coherence radius varied in our calculations nearly from 150 mm for $\beta_0^2 = 10$ to 2–4 mm for $\beta_0^2 = 10000$.

Figure 1 presents 2D scintillation spectra for 12 variants of parameters' values taken for calculations. The product of the wave number by coherence radius is laid off as abscissa, spectral density multiplied by the square of the wave number is laid off as ordinate. For brevity, below it is called the spectrum.

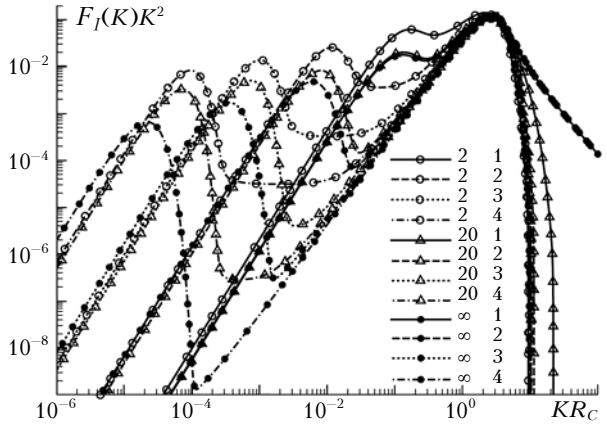

Fig. 1. 2D scintillation spectra for the wave parameter's values $W = 2$, 20, ∞. In the legend, the first number corresponds to W, the second to $\log\beta_0^2$.

In this representation, the area under the curve is proportional to scintillation dispersion. Other 12 calculated variants are intermediate with respect to those presented in Fig. 1.

As is seen in Fig. 1, the spectra have two maxima. The long-wave one is usually called the refraction maximum, and the short-wave one the diffraction maximum. The positions of short-wave maxima on the axis of wave numbers normalized by R_C and their values are close to each other. The spectra for wave parameters W equal to 200 and ∞ in fact coincide for $\beta_0^2 = 10 \div 1000$ before the range of the short-wave maximum. To the right of the short-wave maximum, the spectra with $W = \infty$ differ from others, they are proportional to $(KR_C)^{-5/3}$ for $KR_C \gg 1$. The distance between the positions of maxima is defined mainly by the value of β_0^2. With increase of β_0^2, the distance between the maxima on the axis of wave numbers increases, just as the difference between their amplitudes. The plateau between the maxima appears at $W \le 20$ and broadens with increase of β_0^2. Note that the spectra presented in Fig. 1 agree with the results of Ref. 10 presenting 2D spectra for three values of the internal scale, one of which is zero.

Figure 2 presents the approximation of the 2D spectrum by the equations (7), (8), and (10) with the variant $W = 2$, $\beta_0^2 = 10\,000$ as an example.

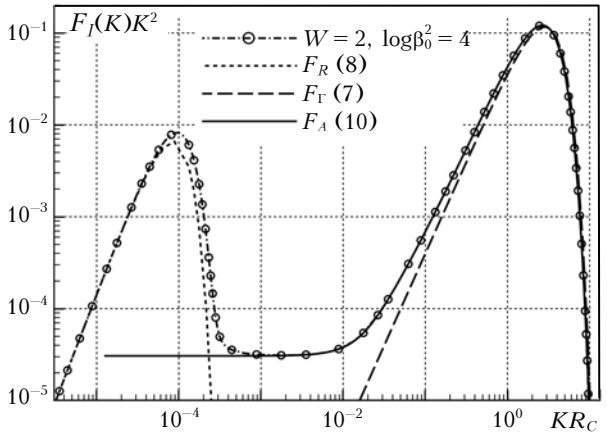

Fig. 2. Analysis of the approximation equations (7), (8), (10) for calculation of 2D spectra with $W = 2$, $\beta_0^2 = 10\,000$ as an example.

The quality of these approximations is visualized in Fig. 3, where the nodes of the grid correspond to parameters' values used in calculations of F_I. The refraction approximation F_R (8) approximates the range of the long-wave maximum. In the maximum, F_R is lower than the exact solution.

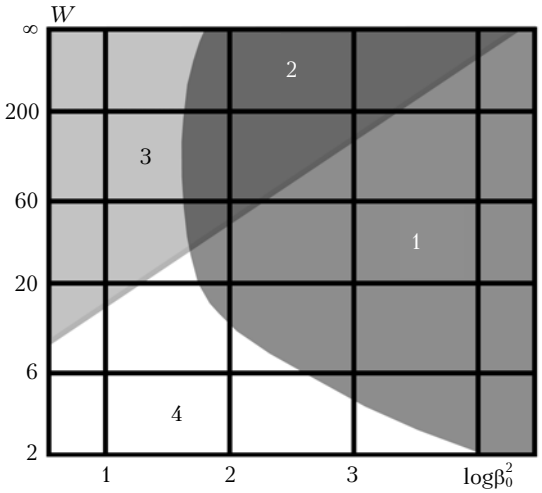

Fig. 3. Zones of applicability for approximations (7), (8), and (10) for the 2D scintillation spectra in the plane of values W and β_0^2. For the long-wave range of the spectrum: 1 and 2 present the F_R approximation (8); for the short-wave range: 2 and 3 present the F_Γ approximation (7), 1 and 4 present the F_A approximation (10).

0235-6880/08/02 96-06 $02.00

The larger are W and β_0^2, the better is the correspondence between F_R and F_I. In zones 1 and 2 in Fig. 3, the relative deviation of F_R from F_I in the maximum does not exceed 20%. The boundary between the nodes of the grid is a broken line, it is smoothed to simplify the interpretation of Fig. 3.

The approximation for the short-wave range of the spectrum, i.e., the spectrum of the squared coherence function F_Γ (7), yields smaller values in the neighborhood of the maximum as compared to the exact solution. The ratio $F_I/F_\Gamma > 1$, which approaches to 1 as approaches to the maximum. The maximum F_Γ is somewhat displaced to the right of the maximum F_I. The larger are W and β_0^2, the less are differences between F_Γ and F_I. The approximation F_A (10), as it is shown in Fig. 2, is closer to the exact solution than F_Γ in a significantly larger interval of wave numbers. This approximation represents the intermediate plateau between these two maxima. Generally, the less is W and larger is β_0^2, the better operates F_A. For the short-wave range in Fig. 3, the approximation F_Γ is closer to the exact solution in zones 2 and 3, the approximation F_A is closer to the exact solution in zones 1 and 4.

Summing the estimates for quality of approximations visually presented in Fig. 3 we see that the 2D spectrum can be represented as a sum of the approximations (8) and (10) in zone 1, a sum of (8) and (7) in zone 2; only (7) operates in zone 3 and only (10) operates in zone 4.

1D scintillation spectra

Figure 4 presents exact solutions for 1D spectra (spectral densities multiplied by the wave number). In Fig. 4*a,* the wave numbers on the abscissa are multiplied by R_C. The general forms of 1D and 2D spectra are similar in this representation. Long-wave and short-wave maxima are also present, and the position of the latter approximately corresponds to Fig. 1: $\kappa_{SW}R_C \sim 1$. Horizontal plateaus, however, are absent. Long-wave maxima are not formed for variants with the minimal value $\beta_0^2 = 10$. In Fig. 4*b,* the 1D spectra are represented as functions of the dimensionless wave number $\kappa R_F^2/R_C$. The long-wave maximums are grouped near the wave number $\kappa_{LW} \approx R_C/R_F^2 \equiv R_C k_0/L$.

Determination of characteristics of the medium by scintillation spectra

To ascertain whether turbulence spectra can be reconstructed, we have analyzed equations connecting properties of the medium and measured spectra. We parameterized the problem because we were interested in the information content of scintillation measurements with respect to parameters characterizing the medium. More refined and exact methods for solving inverse problems are to be analyzed in processing real observations with allowance for their peculiarities. The measurements are performed with restricted exactness, in a bounded range of wave numbers, with interference of real noises. These are the factors that must define the choice of the method for solving the inverse problem. We considered an idealized scheme, in which a particular form of the structural function was used.

For the model (1), scintillation spectra are defined by the following parameters: the distance from the phase screen to the observer L, the efficient structural characteristic of the screen C_{ef}^2, and the wave number κ_m. Let us consider the possibility to define these parameters by the observed 1D spectra under the assumption that the results of calculations can be considered as results of "measurements."

Let the distance L be not known as, for instance, in radio astronomical observations, and let there be two maxima in the observed spectrum, represented as the product of spectral density and the wave number.

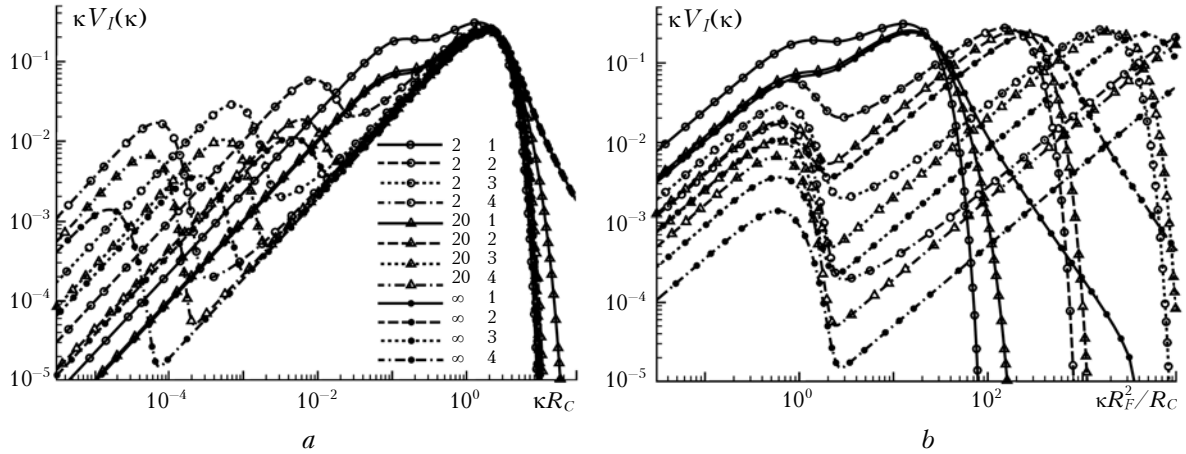

a *b*

Fig. 4. 1D spectra for the values of the wave parameter $W = 2, 20, \infty$. The designations are the same as in Fig. 1: the dimensionless product κR_C (*a*) is laid off on the abscissa; $\kappa R_F^2/R_C$ (*b*).

Then, as follows from the theory[6,22] and analysis of the data presented in Fig. 4, the product of the corresponding wave numbers $\kappa_{LW}\kappa_{SW} \approx k_0/L$ immediately yields an estimate for the distance L:

$$L \approx k_0/(\kappa_{LW}\kappa_{SW}). \qquad (11)$$

The calculations made it possible to determine error of this estimate: it is lower than the exact value of L by 10–20% for $\beta_0^2 \geq 100$.

Then we suppose that the distance L is known, as, for instance, in sensing the Earth's atmosphere from satellites, or its estimate is obtained and a series of models calculated for this L value is available. It remains to find two unknowns, C_{ef}^2 and κ_m. The ratio of positions of the short-wave and long-wave maxima $R\kappa = \kappa_{SW}/\kappa_{LW}$ and that for maxima' amplitudes $RM = V_I(\kappa_{SW})\kappa_{SW}/[V_I(\kappa_{LW})\kappa_{LW}]$ were chosen as spectrum characteristics obtained from observations. We can write two equations for the model (1):

$$f_1(W,\beta_0^2) = R\kappa, \quad f_2(W,\beta_0^2) = RM. \qquad (12)$$

The unknowns C_{ef}^2 and κ_m define W, β_0^2 in Eq. 12 by $W = R_F\kappa_m$ and Eq. (5). The calculated functions f_1 and f_2 are shown in Fig. 5.

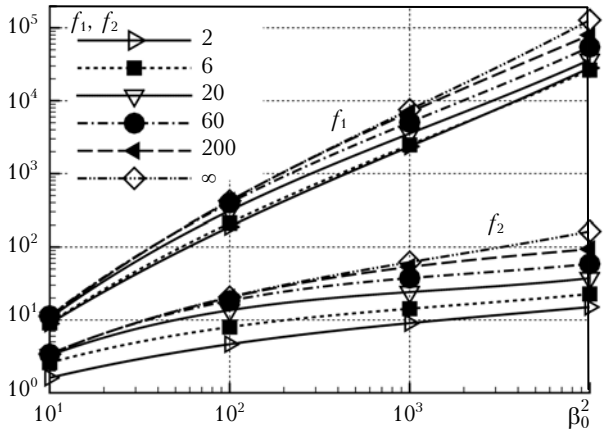

Fig. 5. Functions $f_1(W, \beta_0^2)$ and $f_2(W, \beta_0^2)$. Values of the wave parameter W are presented in the legend.

The equations (12) define two curves in the plane $\{W, \beta_0^2\}$ for the measured values $R\kappa$ and RM. Intersection points of these curves are the solution of the inverse problem. If the angle between tangents to the curves is not small, the error of the solution and the measurement error are of the same order and any serious problems seemingly should not arise in reconstruction of the parameters. If this angle tends to zero, one should use some *a priori* information about the solution. In other words, in order to obtain a reasonable result, one should resort to regularization. Finally, if the curves do not intersect at all in the domain of available measurement data due to, for instance, insufficient resolution of the measurement method, the reconstruction of the whole series of parameters is impossible. In this case, one can hope to reconstruct only one parameter, for instance, C_{ef}^2, assuming κ_m to be *a priori* known.

Figure 6 illustrates position of the curves (12) in the plane $\{W, \beta_0^2\}$ for two examples: when one can solve the inverse problem with small errors and when it is impossible to determine two parameters.

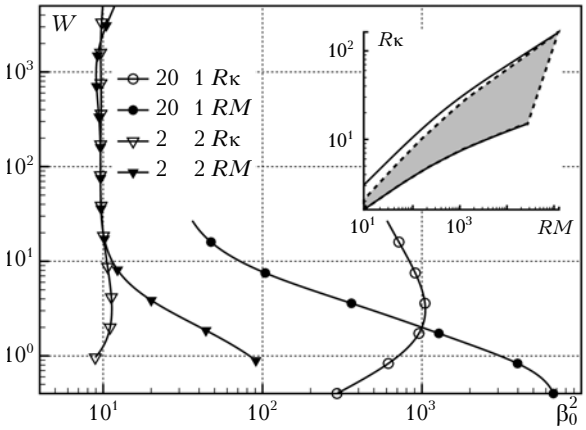

Fig. 6. The curves $f_1(W, \beta_0^2) = R\kappa$ and $f_2(W, \beta_0^2) = RM$ for two examples: $\{W = 20, \log\beta_0^2 = 1, R\kappa = 10.6$ rad/m, $RM = 3.26\}$ and $\{W = 2, \log\beta_0^2 = 2, R\kappa = 190$ rad/m, $RM = 4.65\}$. The shaded zone shows the range of the measured parameters $\{R\kappa, RM\}$, in which the error in reconstructed values is close to the measurement error.

The fragment presents the plane $\{R\kappa, RM\}$ with a mapped zone corresponding to all our "measurements." Based on the analysis of neighborhoods of the intersection points of the curves presented in Fig. 6, we shaded the domain, in which one can expect that the difference between errors of the reconstructed and measured values is not large. Beyond the domain, regularization methods are required to solve the inverse problem. The convenience of this representation is that the parameters $R\kappa$, RM can be obtained from real measurements.

Conclusion

We considered spatial scintillation spectra behind a phase screen with isotropic heterogeneities. The medium that forms the screen was described by a Kolmogorov 3D heterogeneity spectrum including Gaussian attenuation with an internal scale varying from the Fresnel scale to zero. Spectra of strong scintillation were calculated for conditions of optical observations through the Earth's atmosphere from a satellite. The study is based on numerical solution of the equation (2). We studied the dependence of 2D and 1D scintillation spectra on two dimensionless parameters of the problem: the wave parameter $W = \kappa_m\sqrt{L/k_0}$, defined by the internal scale of heterogeneities, and parameter β_0^2, defining scintillation intensity calculated by the perturbation theory.[5] For 2D spectra, domains of applicability of approximate equations (7), (8), (10) were considered. The approximation (10) based on decomposition of

$\Psi(\mathbf{R}, \mathbf{R}')$ by a small $\mathbf{R}$ is shown to be closer to the exact solution in a more wide range of parameters' values as compared to the common approximation of the scintillation spectrum by the spectrum of the squared coherence function.

It is shown that information about parameters of the medium forming the phase screen is contained in observations of 1D spectra of strong scintillation. In the plane $\{R\kappa, RM\}$ we mapped the domain containing the solution of the inverse problem. The solution is stable with respect to measurement errors.

Acknowledgements

The authors thank V.V. Vorob'ev for useful discussions of the obtained results.

This work was supported by the Russian Foundation for Basic Research (Project No. 06–05–64357).

References

1. V.E. Zuev, V.A. Banakh, and V.V. Pokasov, *Optics of the Turbulent Atmosphere* (Gidrometeoizdat, Leningrad, 1988), 270 pp.
2. A.S. Gurvich and V. Kan, Izv. Ros. Akad. Nauk. Ser. Fiz. Atmos. Okeana **39**, No. 3, 335–346 (2003).
3. V.F. Sofieva, A.S. Gurvich, F. Dalaudier, and V. Kan, J. Geophys. Res. **112**, D12113 (2007), doi:10.1029/2006JD007483.
4. A.S. Gurvich, V.V. Vorob'ev, and O.V. Fedorova, Izv. Ros. Akad. Nauk. Ser. Fiz. Atmos. Okeana **42**, No. 4, 502–513 (2006).
5. S.M. Rytov, Yu.A. Kravtsov, and V.I. Tatarskii, *Introduction to Statistical Radiophysics, Part 2* (Nauka, Moscow, 1978), 464 pp.
6. V.I. Shishov, Izv. Vyssh. Uchebn. Zaved. Radiofiz. **14**, No. 1, 85–92 (1971).
7. V.I. Shishov, Izv. Vyssh. Uchebn. Zaved. Radiofiz. **17**, No. 11, 1684–1691 (1974).
8. V.A. Banakh and I.N. Smalikho, Atmos. Oceanic Opt. **6**, No. 4, 233–237 (1993).
9. J. Goodman and R. Narayan, Roy. Astronom. Soc. Monthly Notices **214**, No. 4, 519–537 (1985).
10. J.J. Goodman, R.W. Romani, R.D. Blandford, and R. Narayan, Roy. Astronom. Soc. Monthly Notices **229**, No. 1, 73–102 (1987).
11. V.A. Alimov and A.V. Rakhlin, Izv. Vyssh. Uchebn. Zaved. Radiofiz. **48**, No. 4, 275–282 (2005).
12. V.V. Vorob'ev, D.A. Marakasov, and O.V. Fedorova, Atmos. Oceanic Opt. **19**, No. 12, 900–908 (2006).
13. A.S. Gurvich, V.V. Vorob'ev, D.A. Marakasov, and O.V. Fedorova, Izv. Vyssh. Uchebn. Zaved. Radiofiz. **50**, No. 9 (2007).
14. A.S. Gurvich, V. Kan, S.A. Savchenko, A.I. Pakhomov, P.A. Borovikhin, O.N. Volkov, A.Yu. Kaleri, S.V. Avdeev, V.G. Korzun, G.I. Padalka, and Ya.P. Podvyaznyi, Izv. Ros. Akad. Nauk. Ser. Fiz. Atmos. Okeana **37**, No. 4, 469–486 (2001).
15. S.V. Sokolovskiy, Radio Sci. **35**, No. 1, 95–106 (2000).
16. V. Kan, S.S. Matyugov, and O.I. Yakovlev, Izv. Vyssh. Uchebn. Zaved. Radiofiz. **45**, No. 8, 652–663 (2002).
17. A.S. Gurvich, V. Kan, S.A. Savchenko, A.I. Pakhomov, and G.I. Padalka, Izv. Ros. Akad. Nauk. Ser. Fiz. Atmos. Okeana **37**, No. 4, 487–501 (2001).
18. A.S. Gurvich and V. Kan, Izv. Ross. Akad. Nauk. Ser. Fiz. Atmos. Okeana **39**, No. 3, 347–358 (2003).
19. A. Ishimaru, *Wave Propagation and Scattering in Randomly Heterogeneous Media* [Russian translation] (Mir, Moscow, 1981), 317 pp.
20. V.I. Tatarskii, *Wave Propagation in a Turbulent Atmosphere* (Nauka, Moscow, 1967), 548 pp.
21. I.G. Yakushkin, Izv. Vyssh. Uchebn. Zaved. Radiofiz. **17,** No. 9, 1350–1356 (1974).
22. D.P. Hinson, Radio Sci. **21**, No. 2, 257–270 (1986).